Applied Energy 325 (2022) 119757

Contents lists available at ScienceDirect

Applied Energy

journal homepage: www.elsevier.com/locate/apenergy

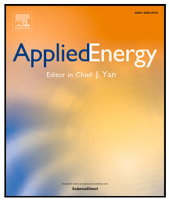

Dynamic *PQ* Operating Envelopes for prosumers in distribution networks

Yasin Zabihinia Gerdroodbari *, Mohsen Khorasany, Reza Razzaghi

Department of Electrical and Computer Systems Engineering, Monash University, Clayton VIC 3800, Australia

ARTICLE INFO

Keywords:
Distributed energy resources
Operating envelopes
Smart grid
Over-voltage
Prosumer

ABSTRACT

The increasing integration of distributed energy resources (DERs) has provided the opportunity to deliver clean, and low-cost power for energy consumers. However, without appropriate coordination, injected power by DERs can violate the operational limits of the electricity distribution networks and cause issues such as over-voltage and lines congestion. Recently, the promising concept of Operating Envelopes (OEs) has been introduced to support the efficient integration of DERs without directly controlling their output. Within this context, this paper presents a novel framework in which prosumers are routinely provided with dynamic active and reactive OEs and can manage their assets accordingly. The network operator in each time step, collects customers' expected export, and considering nodes voltage and lines current limits, calculates the dynamic OEs for each prosumer. Then, an energy management algorithm for prosumers is presented, which enables them to control their PV and battery energy storage system according to their defined *PQ* region. The performance of the proposed framework is evaluated using various simulation studies to demonstrate its significant effectiveness in solving the over-voltage and over-current problems associated with DERs. Furthermore, the comparison of the proposed framework with the state of the art exhibits its superiority in decreasing DERs power curtailment.

1. Introduction

1.1. Background and research motivations

The ongoing adoption of distributed energy resources (DERs) by households and businesses is raising several operational challenges in distribution networks. Distribution network infrastructure has been designed assuming one-way power flow from the upstream network to users at the edge of the grid. However, DERs can result in bidirectional power flows, which can negatively impact power quality in the network [1]. In particular, it can lead to over-voltage [2,3] and congestion (lines over-loading) [4] issues. To resolve these issues, distribution network operators (DNOs) are adopting several solutions which can be classified into two groups. The first group of solutions involves the installation of new equipment such as D-STATCOM (e.g., [5]) or upgrading the existing network elements such as distribution transformer with on-load tap changers (e.g., [6]). There is also another group of solutions in which DNO only manages the DER outputs to resolve network operational issues. Controlling DERs outputs is considered as a low-cost solution since there is no need for new investments to install new devices.

Within the second group, various solutions have been proposed in the recent literature, which can be employed to resolve issues originating from DER integration. These solutions can be further classified in two categories: *(i)* direct control of DERs, by defining their active and reactive setpoints based on the network constraints, *(ii)* indirect control of DERs through either market-based solutions or defining export limits.

Approaches in the first category incorporate network constraints in the control decisions of DERs. In these methods, the network operator or a third party (e.g. an aggregator) is responsible for controlling DERs by adjusting either/both of DERs' output active or/and reactive power reference values. For example, in [7,8], the reactive power capability of DERs for controlling voltage is utilized. These approaches are generally suitable for networks with a low level of DERs penetration or in a network with a low R/X ratio. However, as in general conventional distribution networks have a high R/X ratio, reactive power based compensation strategies are not sufficient as the sole control mechanism in the networks with a high level of DER penetration [9]. Therefore, controlling active power should be an intrinsic part of the control strategy. Methods in [10–12] are mainly based on the control of DERs' active power. By only controlling the output active power, unnecessary curtailment can be imposed on DERs with reactive power control (RPC) capability. The RPC can be complementary even in a network with high R/X ratio. Hence, in order to utilize the full capability of the DERs, the presented methods in some works such as [13–15] control and adjust both active and reactive power output of DERs. This helps to

* Corresponding author.
E-mail addresses: yasin.zabihiniagerdroodbari@monash.edu (Y. Zabihinia Gerdroodbari), mohsen.khorasany@monash.edu (M. Khorasany), reza.razzaghi@monash.edu (R. Razzaghi).

https://doi.org/10.1016/j.apenergy.2022.119757
Received 8 January 2022; Received in revised form 31 May 2022; Accepted 23 July 2022
Available online 13 August 2022

reduce active power curtailment as reactive power compensation is also involved. It should be noted that in general, in these methods, the operation of the distribution system with high DER penetration is modeled, in which the system operator performs a multi-temporal optimal power flow considering specific constraints of DERs and the network. The main drawback of approaches incorporating direct control of DERs is that the DNO should have full access to DERs and network information. This can be unpleasant for DER owners as it violates their privacy.

The second group of studies with indirect control assumes that prosumers (DER owners) use their own energy management system and are responsible to make a decision on managing their assets, while the network operator can only decide on their export limit [16]. The interaction of prosumers and DNO can also be facilitated through an aggregator, in which the aggregator only shares some limited data with the DNO [17]. The indirect control scheme helps prosumers to maintain their privacy by limiting other entities' access to their assets and their detailed demand and generation information. There are few methods that can be employed to set export limits to avoid violating the operational limits in the network. The simplest method, which is currently being implemented by a few network operators (e.g., [18]), is to set region-wide fixed active power export limits at the prosumer connection point. For all prosumers in the network, the limit is identical and the unbalance generation in phases and customers load variation are not taken into account. Hence, such a fixed and region-wide limit in many cases might be too conservative and hinder the full utilization of the network's capacity. Furthermore, it discourages customers from using DER as it diminishes their profitability during demand/generation conditions which does not violate the network constraints.

To resolve these problems, recently the concept of Operating Envelopes (OEs) has been gaining attention and trialled by network operators in Australia [19–22]. As defined in [19] "an OE is a principled allocation of the available hosting capacity to the individuals or aggregate DER or connection points within a segment of a distribution network in each time interval". DNOs employ OEs to determine prosumers' import or export power limits which they must follow to ensure the network integrity. The OEs can be defined to tackle one or multiple operating challenges, such as voltage regulation and congestion. OEs can also be utilized by aggregators to coordinate DERs for participation in energy and frequency control ancillary service (FCAS) markets [22]. Through using OEs for each prosumer, the unnecessary curtailment can be avoided, which in turn increases green energy utilization in the network. Furthermore, the DNO can harvest more power from the network and utilize the network's hosting capacity more efficiently.

The OEs can be implemented using different frameworks for standalone or aggregated DERs. For the aggregated DERs, the DNO communicates with an aggregator to calculate OEs, while the aggregator has communication with prosumers and controls their assets. This scheme can be seen in [17,21,23]. The OEs can also be directly communicated to prosumers, such that the DNO calculates the OEs and send them to prosumers. Then, the prosumers manage their assets individually [24]. The main difference between these two schemes is that in the first one a third party controls the prosumers while in the second one they have a standalone operation. Furthermore, in terms of data sharing frequency, the OEs can be calculated either in the day-ahead (offline) or near real-time (online). The day-ahead calculation uses forecast of load and generation [23], while in the online calculation, the DNO collects the data from the aggregator or prosumers in each time interval. The dynamic data sharing will have more accuracy as in low-voltage distribution networks accurate load forecasting is challenging [25]. Also, dynamic data sharing allows to adjust the calculated OEs through iterative negotiations as presented in [17]. However, as the number of prosumers in distribution networks is generally high, calculating OEs should be computationally efficient and scalable to make the online calculation process practical.

The DNO can provide prosumers/aggregator with two types of OEs: *(i)* active power OEs, *(ii)* active and reactive power OEs. In the first type, the DNO calculates a limit for prosumers' active power generation with respect to their intended operation power. The active power-based OEs improve system integrity by avoiding the violation of voltage or lines thermal constraints as demonstrated in [17,23,24]. However, neglecting reactive power in OE calculation might result in conservative results, and by defining OEs for both active and reactive power, more potential values for DER owners can be unlocked. This is in line with the recent growth in the installation of smart DERs equipped with RPC functionality in countries such as Australia, where the industrial projects are also involving the reactive power in the control of DERs [26,27]. For example, [26] investigates the adoption of traditional approaches to improve distribution networks hosting capacity considering the recommended *Volt-Watt* and *Volt-var* settings [28]. The summary of different methods and the relevant references have been presented in Table 1.

1.2. Contributions

In this paper, a novel approach for the calculation of dynamic active and reactive power OEs for DERs is proposed. The proposed approach allows prosumers to independently manage their assets based on their preferences without the direct involvement of any third party (e.g. DNO or aggregator). This results in preserving the DER owners privacy by avoiding the full access of DNO to the assets information and detailed demand/generation data. In the proposed method, the DNO defines prosumers' OEs for each time interval based on their expected power and network conditions. Compared to the existing region-wide fixed active power limits, the dynamic calculation of OE results in avoiding unnecessarily curtailing of the DER power exports to the network. Furthermore, in contrast to active power based OEs, the proposed method determines the OEs in the *PQ* region and fully exploits the reactive power capability of smart inverters. This can brings more profitability to DER owners and higher distributed generation in the network. In summary, the main features of the proposed methodology compared to the stat of the art are as follows:

- Considers both active and reactive power limits, which enables prosumers with RPC capability to control their active and reactive power optimally, enabling them to potentially export more active power;
- It is highly scalable and an increase in the number of customers and prosumers does not change the OEs computation time significantly;

The rest of this paper is organized as follows; the system model and the proposed methodology for calculating OE are presented in Section 2, followed by the details of DNO and prosumers algorithms in Section 3. Section 4 presents the results of the proposed approach. Section 5 presents a comparative analysis with the state of art. Finally, the concluding remarks are outlined in Section 6.

2. The proposed dynamic operating envelop

2.1. System model

As shown in Fig. 1, in this paper a three-phase 4-wire, low-voltage distribution network is considered. The network $\mathcal{G}(\mathcal{N},\mathcal{L})$ consists of a set of nodes with index $n \in \mathcal{N}$ and a set of lines with index $l \in \mathcal{L}$ connecting these nodes. The network includes ($h \in \mathcal{H}$) customers connected between a phase and neutral where their phase connection is denoted as ϕ^h. Besides load, customers can be equipped with a PV solar system (PVSS) and battery energy storage system (BESS). These customers are identified as prosumers, while the ones with only load are considered as consumers. $\mathcal{H}_v^t$ is the set of prosumers that are going to be provided with OEs at t, whereas $\mathcal{H}_f^t$ is the set of consumers as well as prosumers that are going to export their expected power. In the rest of the paper, members of $\mathcal{H}_v^t$ and $\mathcal{H}_f^t$ are denoted as prosumers with

Table 1
Summary of different methods for DER control.

		Direct control		Indirect control		Online calculation
		P	Q	P	Q	
Methods	[7,8]		✓			✓
	[10–12]	✓				✓
	[13–15]	✓	✓			✓
	[17,24]			✓		✓
	[23]			✓		
	The proposed methodology			✓	✓	✓

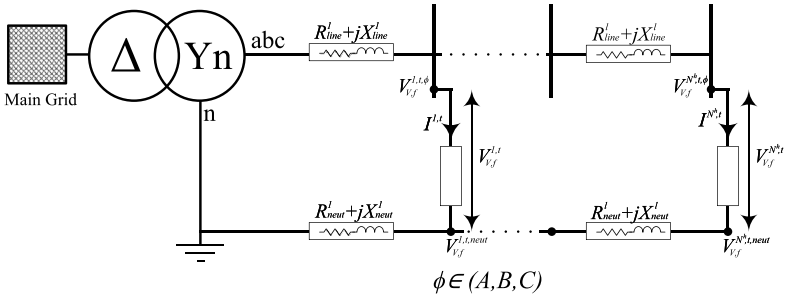

Fig. 1. A 4-wire 3-phase radial low-voltage distribution network.

OE (PWOE), and customers with fixed power (CWFP), respectively. The formation of these sets in each time slot is further explained in Section 3.1.

Prosumers can use energy from their PVSS and BESS or the grid to meet their demand. If they have surplus power, it can be used to charge the battery or to be injected into the grid. In time slot t, the injected power by each prosumer is calculated as:

$$P^{h,t} = P^{h,t}_{pv} + P^{h,t}_{d} - P^{h,t}_{ld} - P^{h,t}_{c} \tag{1}$$

$$Q^{h,t} = Q^{h,t}_{pv} - Q^{h,t}_{ld} \tag{2}$$

where, $P^{h,t}_{pv}/Q^{h,t}_{pv}$ and $P^{h,t}_{ld}/Q^{h,t}_{ld}$ denote the generated active/reactive power by PV, and the active/reactive power demand of prosumer h, respectively. Positive values of $P^{h,t}/Q^{h,t}$ denote the injected power by the prosumer, while the negative values indicate the absorbed power. Furthermore, the charging and discharging power are denoted as $P^{h,t}_{c}$, and $P^{h,t}_{d}$, respectively which should be less than the maximum possible charging/discharging power:

$$P^{h,t}_{c} \le \overline{P}^{h}_{c}, \quad P^{h,t}_{d} \le \overline{P}^{h}_{d}. \tag{3}$$

The State of Charge (SoC) of the battery at time t is given by (4), which should be constrained by (5) to reduce the battery degradation [29]:

$$\sigma^{h,t} = \sigma^{h,t-1} + (P^{h,t}_{c}\eta^{h}_{c} - P^{h,t}_{d}/\eta^{h}_{d})\frac{\Delta t}{\overline{E}^{h}} \tag{4}$$

$$\underline{\sigma}^{h} \le \sigma^{h,t} \le \overline{\sigma}^{h} \tag{5}$$

where $\overline{E}^{h}$ is the capacity of the prosumer's BESS, and Δt is the duration of each time interval. The amount of active and reactive power that prosumer can inject/absorb are bounded by the OEs ($OE^{h,t}$) issued by the DNO as in (6). The procedure for calculating these envelopes is explained in Sections 2.2 and 3.

$$\left(P^{h,t}, Q^{h,t}\right) \in OE^{h,t} \tag{6}$$

2.2. Dynamic operating envelop calculation

The OE of a prosumer in a time interval includes multiple operating regions. It consists of voltage safe operating region (VSOR) and current safe operating region (CSOR). The final OE is the intersection of all these regions (see Fig. 2). In the following, the procedure of calculating prosumers' VSOR and CSOR have been explained. It should be noted that as the focus of this paper is on the negative impact of DER integration, the calculations are for prosumers' generation.

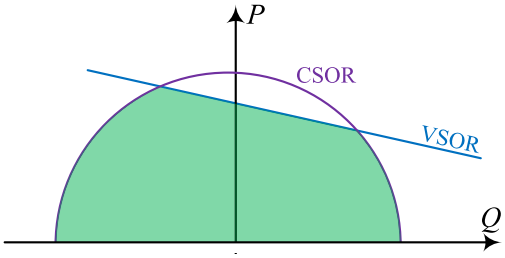

Fig. 2. The proposed OE scheme as the intersection of CSOR and VSOR.

2.2.1. VSOR

In the calculation of prosumers' VSOR, since the maximum voltage in each phase at t happens, in general, at the last generating prosumers (a^t, b^t, and c^t in phase A, B, and C, respectively), their voltage magnitude are used as the reference.[1] In a three-phase four-wire LVDN, their voltage magnitude change can be calculated by [30]

$$\Delta V^{k,t} = \Delta V^{k,t}_{v} + \Delta V^{k,t}_{f} \quad (k \in \{a^t, b^t, c^t\}), \tag{7}$$

where

$$\Delta V^{k,t}_{v,f} \approx \sum_{h \in \mathcal{H}^{t}_{v,f}} \left(cos(\phi^{k} - \phi^{h})R^{kh} + sin(\phi^{k} - \phi^{h})X^{kh}\right)P^{h,t}_{v,f} + \left(-sin(\phi^{k} - \phi^{h})R^{kh} + cos(\phi^{k} - \phi^{h})X^{kh}\right)Q^{h,t}_{v,f}. \tag{8}$$

$\Delta V^{k,t}_{v}$ and $\Delta V^{k,t}_{f}$ are the resulted voltage change of prosumer k caused by PWOE and CWFP, respectively. Moreover, R^{kh} and X^{kh} are the mutual resistance and reactance between costumer k and h, respectively. For network of Fig. 1 they can be calculated by

$$R^{kh} = R^{kh}_{line} + R^{kh}_{neut}, \tag{9}$$

[1] It should be noted that the power-flow analysis can also be used to identify these prosumers.

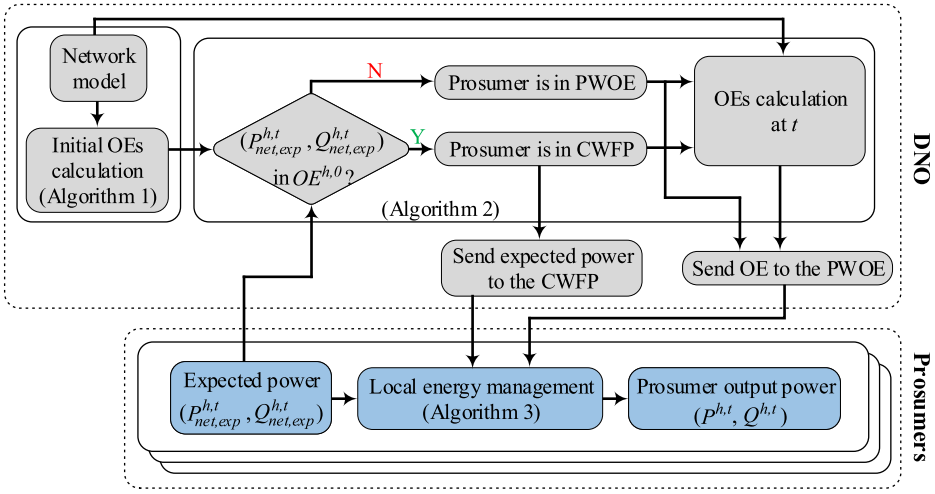

Fig. 3. Overview of the proposed control framework.

$$X^{k,h} = X^{k,h}_{line} + X^{k,h}_{neut}. \tag{10}$$

$R^{k,h}_{line}$ and $X^{k,h}_{line}$ are the resistance and reactance of the common path between the costumers k and h to the slack bus through the phase wires, respectively. It is 0 if k and h are connected to the different phases. Furthermore, $R^{k,h}_{neut}$ and $X^{k,h}_{neut}$ are the resistance and reactance of the common path between the customers k and h to the slack bus by the neutral wire, respectively. $R^{k,h}_{neut}$ and $X^{k,h}_{neut}$ are always positive as all customers are single-phase and connected to the neutral. It should be noted that (7) and (8) represent the real part of the voltage change of prosumer k. This is due to the fact that in a conventional low-voltage distribution network, the voltage phase change is insignificant.

In order to utilize the full capacity of the network, if all PWOE select their active and reactive power from their boundary, the maximum voltage change of prosumers a^t, b^t, and c^t should be $\Delta\overline{V}$. $\Delta\overline{V}$ is the allowed voltage rise determined by the DNO. Furthermore, the defined VSOR for PWOE connected to the same phase should be similar to have a fair contribution to avoid over-voltage problems. Therefore, the boundary of VSOR can be estimated as a line, in which $P^{\phi,t}_0$ and $Q^{\phi,t}_0$ are its P and Q axis intercepts, respectively ($\phi \in \{A, B, C\}$). To calculate $P^{\phi,t}_0$ and $Q^{\phi,t}_0$, (7) can be rewritten as:

$$\Delta V^{k,t}_v = \Delta\overline{V} - \Delta V^{k,t}_f, \tag{11}$$

where $\Delta V^{k,t}_f$ is the same as (8), while $\Delta V^{k,t}_v$ is

$$\begin{aligned}\Delta V^{k,t}_v \approx \sum_{h\in\mathcal{H}^t_v} &\big(cos(\phi^k-\phi^h)R^{k,h} + sin(\phi^k-\phi^h)X^{k,h}\big)P^{\phi,t}_0 + \\ &\big(-sin(\phi^k-\phi^h)R^{k,h} + cos(\phi^k-\phi^h)X^{k,h}\big)Q^{\phi,t}_0.\end{aligned} \tag{12}$$

This is a 3×3 system of linear equations, in which by selecting $Q^{\phi,t}_0 = 0$ and $P^{\phi,t} = 0$, the $P^{\phi,t}_0$ and $Q^{\phi,t}_0$ can be obtained, respectively. Therefore, VSOR of the prosumer h connected to phase ϕ is

$$P^{h,t}_v \le (-P^{\phi,t}_0/Q^{\phi,t}_0)Q^{h,t}_v + P^{\phi,t}_0. \tag{13}$$

2.2.2. CSOR

In order to avoid congestion in line $l \in \mathcal{L}$, it is considered that lines losses are negligible compared to the total transmitting power, and the voltage across a line does not change significantly compared to their nominal value. Hence, one can get

$$\sqrt{\Big(\sum_{h\in\mathcal{H}^{l,t}_v} P^{h,t}_v + \sum_{h\in\mathcal{H}^{l,t}_f} P^{h,t}_f\Big)^2 + \Big(\sum_{h\in\mathcal{H}^{l,t}_v} Q^{h,t}_v + \sum_{h\in\mathcal{H}^{l,t}_f} Q^{h,t}_f\Big)^2} \le S^l_{max}, \tag{14}$$

where S^l_{max} is the line l capacity, $\mathcal{H}^{l,t}_v$ and $\mathcal{H}^{l,t}_f$ are the set of PWOE and CWFP that inject power into the line l, respectively. The defined CSOR for all PWOE should be the same to enable their equitable participation in avoiding over-current condition. Therefore, (14) can be rewritten as (15) to obtain CSOR of customer $h \in \mathcal{H}^{l,t}_v$ for line l:

$$(|\mathcal{H}^{l,t}_v|P^{h,t}_v + \sum_{h\in\mathcal{H}^{l,t}_f} P^{h,t}_f)^2 + (|\mathcal{H}^{l,t}_v|Q^{h,t}_v + \sum_{h\in\mathcal{H}^{l,t}_f} Q^{h,t}_f)^2 \le {S^l_{max}}^2, \tag{15}$$

where $|\mathcal{H}^{l,t}_v|$ is the number of customers in set $\mathcal{H}^{l,t}_v$. It can be seen that (15) is a circle equation as the line loading is only dependent on the magnitude of the apparent power it transmits. Furthermore, since a PWOE contribute in loading of multiple lines ($\mathcal{L}^h$), it has a CSOR per line in which its power passes through.

3. The interaction of DNO and prosumers

Fig. 3 shows the interaction of DNO with prosumers which shows how they perform their algorithms in each time slot. The process starts with DNO calculating initial OEs based on the network model and customer types (Algorithm 1). In the next step, the DNO uses the initial OEs and the expected power output of prosumers to calculate the final OEs (Algorithm 2). Then, prosumers receive the calculated OEs and perform their energy management algorithm to operate their

Algorithm 1 Initial OEs Calculation

Input: $\mathcal{G}(\mathcal{H},\mathcal{L})$, $\mathcal{L}^h$ ($\forall h \in \mathcal{H}$), $\mathcal{H}^0_v$, $\mathcal{H}^0_f$
for $l \in \mathcal{L}$ **do**
  Form $\mathcal{H}^{l,0}_v$ and $\mathcal{H}^{l,0}_f$ using $\mathcal{G}(\mathcal{H},\mathcal{L})$, $\mathcal{H}^0_v$, and $\mathcal{H}^0_f$
end for
$P^{h,0}_f = 0$, $Q^{h,0}_f = 0$ ($\forall h \in \mathcal{H}^0_f$)
$OE^{h,0} = \{\}$ ($\forall h \in \mathcal{H}^0_v$)
Calculate $P^{\phi,0}_0$ and $Q^{\phi,0}_0$ by solving (11) ($\phi \in \{A, B, C\}$)
for $h \in \mathcal{H}^0_v$ **do**
  Calculate VSOR of h connected to phase ϕ using (13), and append it to $OE^{h,0}$
end for
for $h \in \mathcal{H}^0_v$ **do**
  for $l \in \mathcal{L}^h$ **do**
    Calculate CSOR of h for line l using (15), and append it to $OE^{h,0}$
  end for
end for
Output: $OE^{h,0}$ ($\forall h \in \mathcal{H}^0_v$), $\mathcal{H}^{l,0}_v$, and $\mathcal{H}^{l,0}_f$

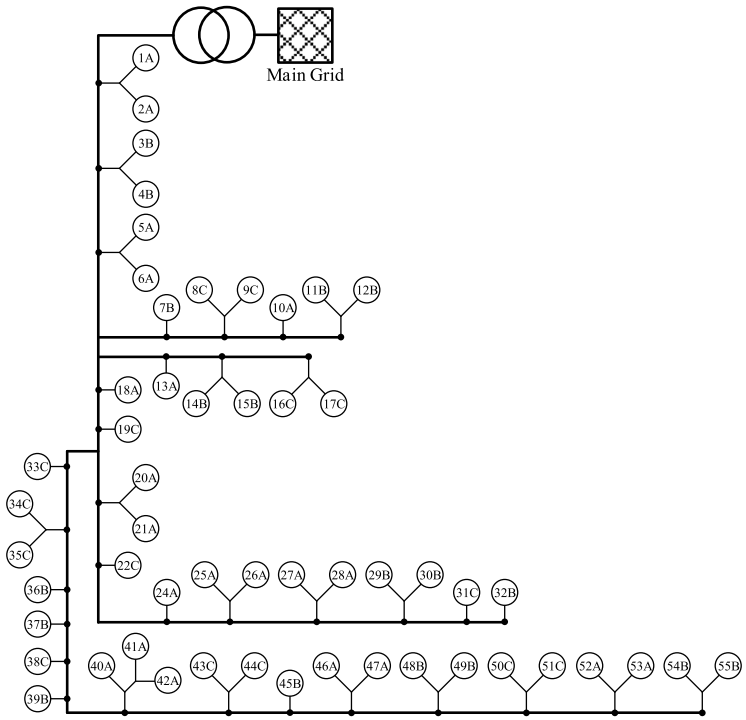

Fig. 4. IEEE European low-voltage test feeder.

assets within the defined OEs (Algorithm 3). The DNO and prosumers algorithms have been further explained in the rest of this section.

3.1. DNO algorithm

The DNO aims to provide prosumers with OEs to ensure all the network constraints are respected. To this end, the DNO performs a two-step algorithm. In the first step, it calculates prosumers initial OEs which will be later used to form $\mathcal{H}_v^t$ and $\mathcal{H}_f^t$. Then, according to these new sets, in the second step, it calculates the updated OEs.

3.1.1. Step 1: Calculating initial OEs

In the calculation of initial OEs ($OE^{h,0}$), only customers' types are considered, whether they are prosumer or consumer. Furthermore, loads are considered 0, the power of consumers is 0. Hence, in this condition, the calculated OEs are only based on the network's hosting capacity. In Algorithm 1, the process of calculating the $OE^{h,0}$ is illustrated. $\mathcal{H}_v^0$ and $\mathcal{H}_f^0$ are the set of PWOE and CWFP. If a customer is a prosumer, it is a member of $\mathcal{H}_v^0$, otherwise it is a member of $\mathcal{H}_f^0$. Consequently $\mathcal{H}_v^{l,0}$ and $\mathcal{H}_f^{l,0}$ ($l \in \mathcal{L}$) can be formed. Then, the OEs according to Sections 2.2.1 and 2.2.2 are calculated. It should be noted that this algorithm is only required to be performed once provided the network topology remains unchanged. In the case of any change such as installing a new PVSS or a change in lines impedance, the initial OEs need to be updated.

3.1.2. Step 2: Calculating updated OEs

After calculating the initial OEs, the DNO calculates the updated OEs using Algorithm 2. This algorithm is performed by DNO in each time step to provides prosumers with the OEs, so that they are able to perform their energy management algorithm. In this algorithm besides the network model, the main inputs are initial OEs and customers expected output power, $P_{net,exp}^{h,t}$ and $Q_{net,exp}^{h,t}$ (collected in advance). If a prosumer's expected power satisfies its initial OE, it means that its power is within the network's hosting capability. Therefore, it does not need to be curtailed and it is appointed as a CWFP. Accordingly, sets $\mathcal{H}_v^0$, $\mathcal{H}_v^{l,0}$, $\mathcal{H}_f^0$ and $\mathcal{H}_f^{l,0}$ are updated to $\mathcal{H}_v^t$, $\mathcal{H}_v^{l,t}$, $\mathcal{H}_f^t$ and $\mathcal{H}_f^{l,t}$. Then, similar to Algorithm 1, the OEs at t are calculated. The DNO dispatches these OEs to the customers in $\mathcal{H}_v^t$, while the CWFP receive their expected power.

Algorithm 2 DNO Main Algorithm at t

Input: $\mathcal{G}(\mathcal{H},\mathcal{L})$, $\mathcal{L}^h$ ($\forall h \in \mathcal{H}$), $OE^{h,0}$ ($\forall h \in \mathcal{H}_v^0$), $\mathcal{H}_v^0$, $\mathcal{H}_f^0$, $P_{net,exp}^{h,t}$, and $Q_{net,exp}^{h,t}$
$\mathcal{H}_v^t = \{\}$, $\mathcal{H}_f^t = \mathcal{H}_f^0$
for $h \in \mathcal{H}_v^0$ **do**
  if $\left(P_{net,exp}^{h,t}, Q_{net,exp}^{h,t}\right) \in OE^{h,0}$ **then**
    Append h to $\mathcal{H}_f^t$
  else
    Append h to $\mathcal{H}_v^t$
  end if
end for
for $l \in \mathcal{L}$ **do**
  Form $\mathcal{H}_v^{l,t}$ and $\mathcal{H}_f^{l,t}$ using $\mathcal{G}(\mathcal{H},\mathcal{L})$, $\mathcal{H}_v^t$, and $\mathcal{H}_f^t$
end for
$P_f^{h,t} = P_{net,exp}^{h,t}$, $Q_f^{h,t} = Q_{net,exp}^{h,t}$ ($\forall h \in \mathcal{H}_f^t$)
$OE^{h,t} = \{\}$ ($\forall h \in \mathcal{H}_v^t$)
Calculate $P_0^{\phi,t}$ and $Q_0^{\phi,t}$ by solving (11) ($\phi \in \{A, B, C\}$)
for $h \in \mathcal{H}_v^t$ **do**
  Calculate VSOR of h connected to phase ϕ using (13), and append it to $OE^{h,t}$
end for
for $h \in \mathcal{H}_v^t$ **do**
  for $l \in \mathcal{L}^h$ **do**
    Calculate CSOR of h for line l using (15), and append it to $OE^{h,t}$
  end for
end for
Output: $OE^{h,t}$ ($\forall h \in \mathcal{H}_v^t$), and $[P_f^{h,t}, Q_f^{h,t}]$ ($\forall h \in \mathcal{H}_f^t$)

Table 2
Location and size of PVSSs in Case Study 1.

P_n (kW)	Houses no.
3.0	1A*, 4B*, 5A, 13A, 16C, 24A*, 26A, 27A, 30B*, 33C, 39B, 41A, 45B*, 48B*, 50C, 51C*, 54B
4.0	7B, 9C, 10A, 11B, 14B*, 19C*, 21A, 28A*, 31C, 32B*, 38C*, 42A*, 44C*, 49B
5.0	3B, 6A*, 8C*, 12B*, 17C*, 18A*, 20A*, 22C*, 23B 25A*, 29B*, 34C*,36B*, 40A*, 43C, 46A*, 52A*, 53A*, 55B*

Table 3
Location, capacity and the maximum charging/discharging power of BESSs in Case Study 1.

Capacity (kWh), P_c^{max}/P_d^{max} (kW)	Houses no.
3.3, 2.0	1A, 24A, 45B, 54B
6.5, 3.0	11B, 19C, 28A, 31C, 32B, 36B
9.8, 4.0	6A, 8C, 17C, 40A, 52A

Table 4
Summary of simulation *Case Study 1* and *Case Study 2*.

	Unlimited	Fixed limit	Proposed framework
Total generated active power (MWh)	1.312	0.976	1.109
No. of customers with OV	26	1	0
No. of lines with OC	6	0	0

3.2. Prosumers' algorithm

The main focus of this paper is to propose a methodology to calculate dynamic active and reactive OEs to avoid voltage and congestion problems. This has been presented in Sections 2 and 3.1. In order to show how prosumers can incorporate these OEs in their energy management algorithm, in this section, an algorithm is presented that each prosumer uses to manage its resources optimally, taking into account the OEs issued by the DNO.

Algorithm 3 Prosumer Algorithm

Input: $OE^{h,t}$
Calculate $\overline{Q}^{h,t}$ using (18)
Calculate $P_{net}^{h,t}$, $\overline{P}_{OE}^{h,t}$, and $P_{cur}^{h,t}$
if $P_{net}^{h,t} > 0$ **then**
  if $\sigma^{h,t} < \overline{\sigma}^{h}$ **then**
    Calculate the charging power using (19)
    Update SoC using (4)
    Calculate injected power using (20)
  else
    $\sigma^{h,t} = \sigma^{h,t-1}$
    Calculate injected power using (21)
  end if
  $Q^{h,t}$ = minimum reactive power at $P^{h,t}$
else if $P_{net}^{h,t} \le 0$ **then**
  if $\sigma^{h,t} > \underline{\sigma}^{h}$ **then**
    Calculate the discharging power using (22)
    Update SoC using (4)
    Calculate absorbed power using (23)
  else
    $\sigma^{h,t} = \sigma^{h,t-1}$
    $P^{h,t} = P_{net}^{h,t}$
  end if
  $Q^{h,t} = Q_{ld}^{h,t}$
end if
Output: $P^{h,t}, Q^{h,t}$

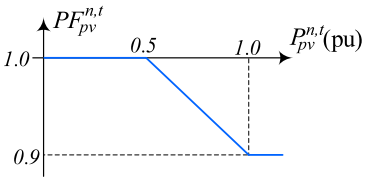

Fig. 5. The $cos(\phi)$ droop control.

It is assumed that prosumers buy energy from retailers at predefined rates (e.g. time of use tariff) and sell energy to the grid at a fixed rate (feed-in-tariff), and the buying price is always higher than the selling price. Hence, since the energy from PVSS is free, each prosumer first uses this energy to meet its demand. The net energy (expected power) of each prosumer h at time t is

$$P_{net}^{h,t} = P_{pv}^{h,t} - P_{ld}^{h,t}. \tag{16}$$

If $P_{net}^{h,t} > 0$, the prosumer has excess power which can be stored in the battery or be injected into the grid. In this condition, the curtailed active power with respect to the provided OE is

$$P_{cur}^{h,t} = \max\,[0, P_{net}^{h,t} - \overline{P}_{OE}^{h,t}], \tag{17}$$

where $\overline{P}_{OE}^{h,t}$ is the maximum allowed active power export by the OE with respect to the maximum reactive power capability of prosumers ($\overline{Q}^{h,t}$). If $P_{net}^{h,t}$ is greater than this value, the prosumer must curtail ($P_{cur}^{h,t} > 0$). Otherwise, it is 0 and $P_{net}^{h,t}$ is within $OE^{h,t}$. $\overline{Q}^{h,t}$ can be also determined by

$$\overline{Q}^{h,t} = Q_{ld}^{h,t} + P_{pv}^{h,t} \times \tan(\cos^{-1}(\underline{PF})), \tag{18}$$

where $\underline{PF}$ is the minimum allowed operating power factor by the DNO [15].

If the battery is not full, the prosumer charges its battery with the excess power considering the maximum charging limit using (19)

$$P_c^{h,t} = \min\,[P_{net}^{h,t}, P_{cur}^{h,t} + k^h \overline{P}_c^h, \overline{P}_c^h, \frac{\overline{E}^h}{\Delta t}(\overline{\sigma}^h - \sigma^{h,t-1})] \tag{19}$$

and the SoC will be updated using (4). Then, if there is remaining power, it will be injected to the grid up to the allowable limit by OE,

$$P^{h,t} = \min\,[P_{net}^{h,t} - P_c^{h,t}, \overline{P}_{OE}^{h,t}]. \tag{20}$$

If the battery is full, all of the excess power will be injected to the grid considering the OE,

$$P^{h,t} = \min\,[P_{net}^{h,t}, \overline{P}_{OE}^{h,t}]. \tag{21}$$

After obtaining the active power, the reactive power is the minimum reactive power at $P^{h,t}$ according to $OE^{h,t}$.

If $P_{net}^{h,t} < 0$, the prosumer needs to discharge its battery or absorb power from the grid. The stored energy in the battery is reasonably cheaper than the grid's energy. Hence, it is reasonable to assume that each prosumer first uses its battery to meet the demand [31]. Therefore, if the battery is not empty, it will be discharged to meet the demand. The amount of discharged power is calculated based on the SoC and the maximum discharge limit as in (22)

$$P_d^{h,t} = \min\,[|P_{net}^{h,t}| + k^h \overline{P}_d^h, \overline{P}_d^h, \frac{\overline{E}^h}{\Delta t}(\sigma^{h,t-1} - \underline{\sigma}^h)] \tag{22}$$

The SoC will be updated using (4), and the requested power from the grid can be calculated by

$$P^{h,t} = P_{net}^{h,t} + P_d^{h,t} \tag{23}$$

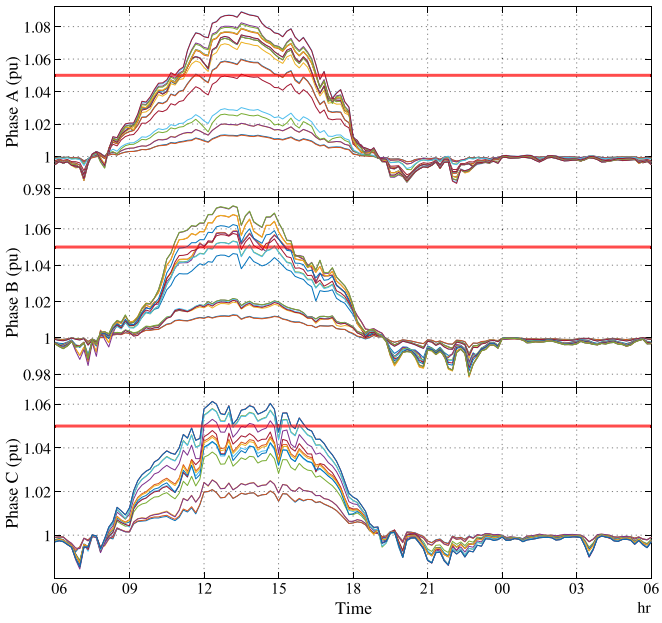

Fig. 6. Customers voltage magnitude when there is not any operational limit.

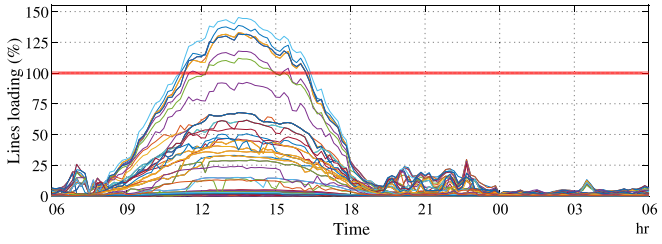

Fig. 7. Lines loading magnitude when there is not any operational limit.

In case the battery is uncharged, the prosumer apply its requested power from the grid, $P^{h,t} = P^{h,t}_{net}$. Furthermore, the prosumer's reactive power when $P^{h,t}_{net} < 0$ is $Q^{h,t} = Q^{h,t}_{ld}$

The pseudocode of the prosumer's algorithm is provided in Algorithm 3. It should be noted that in (19) and (22), k^h is the coefficient that prosumer h uses to make sure that BESS is going to be fully charged during the day and fully discharged during the night. A sensitivity analysis on its impact on the performance of the prosumer's algorithm is presented in Section 4.4.

4. Simulation studies

The performance of the proposed approach is evaluated using the IEEE European low-voltage test feeder [32] shown in Fig. 4. To this end, Python and DIgSILENT PowerFactory are used to implement the control framework, and to perform time series (Quasi-Dynamic) 3-phase 4-wire power flow analysis. Four simulation case studies have been reported:

- The effectiveness of the proposed strategy on a network with a high level of PVSSs penetration has been studied;
- It is compared with the conventional fixed limit active power generation approach to illustrate its advantages.
- The scalability of DNO's algorithm has been investigated;
- A sensitivity analysis on different values on k and its impact on the performance of prosumers algorithm is carried out.

It should be noted that in these studies the defined upper limit for voltage magnitude is considered as 1.05 pu according to ANSI C84.1 [33]. The control inputs k^h and $\underline{PF}$ (in studies in which OEs are provided)

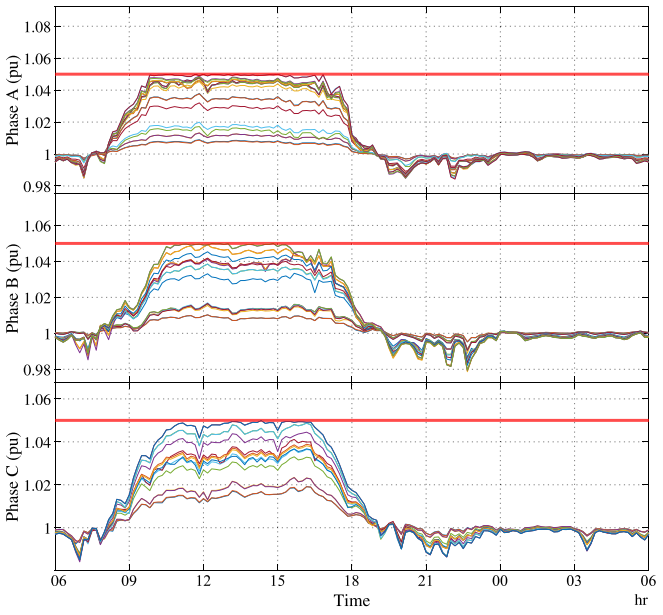

Fig. 8. Customers voltage magnitude when prosumers are provided with OEs.

are set to 0.1 and 0.9, respectively. In addition, the time discretization is 10 min.

4.1. Case study 1: PV-rich network

In this case study, it is considered that 50 out of 55 houses are equipped with PVSSs with the nominal capacity of 3, 4, and 5 kW (Table 2). Some of these PVSSs are able to support RPC and are oversized by 10% (denoted by "*" in Table 2). Moreover, 15 of houses with PVSSs are also equipped with BESSs. Their location, capacity, and the maximum charging/discharging power can be seen in Table 3, adapted from [34]. Furthermore, in order to evaluate the effectiveness of the proposed framework in the case of worse over-voltage and over-current conditions, cable "4c .1" and "4c .06" are replaced with cable "35 SAC XSC". Other data and parameters of the network are provided in [32] and are not reported here.

4.1.1. Network's performance

First, the performance of the network is studied when there is no export limit. In this condition, the prosumer algorithm (Algorithm 3) does not change except that prosumers with reactive power capability control their output reactive power according to $cos(\phi)$ droop control (Fig. 5), adopted from AS/NZS 4777.2 [35]. Also, prosumers with BESS charge using the surplus power.

Figs. 6 and 7 show the voltage magnitude of customers in each phase and lines loading, respectively. As it can be seen form the results, multiple customers face over-voltage, such that some customers' voltage in phase A overpass 50% above the defined limit (1.05 pu). In parallel, a few lines also experience over-current which can primarily result in their overheating. This situation happens despite the presence of a few prosumers with BESSs. Furthermore, PVSSs' RPC is not sufficient due to the large R/X ratio of cables and lines in distribution grids.

By providing prosumers with the proposed dynamic OEs, the performance of the network improves noticeably. As shown in Figs. 8 and 9, there is not any over-voltage problem in the network and all lines operate within a safe loading. In addition, although the phase voltage unbalance factor (calculated using the method explained in Appendix) is not considered in the OEs calculation, since the voltage magnitude of all nodes is limited to 1.05 pu, the unbalance factor is reduced significantly during the peak generation (see Fig. 10).

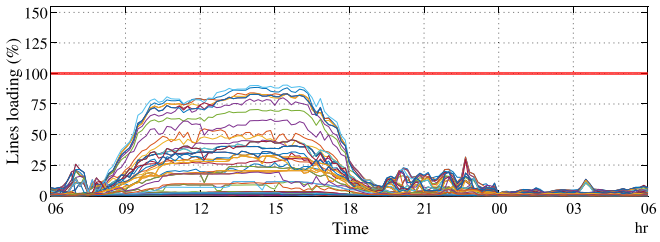

Fig. 9. Lines loading magnitude when prosumers are provided with OEs.

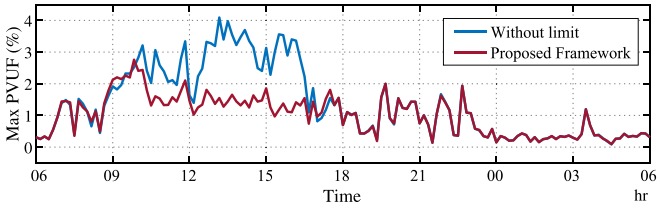

Fig. 10. Maximum phase voltage unbalance factor of the network when prosumers are/are not provided with OEs.

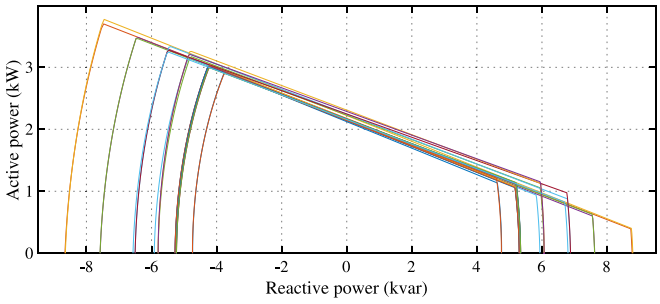

Fig. 11. Prosumer 40A's OEs.

4.1.2. Prosumers' performance

Figs. 11 and 12 depict the intersection of provided VSOR and CSORs to the prosumer 40A and its active and reactive power, respectively. As shown, besides the OEs limit the output active power, the excessive reactive power compensation is also bounded. This can be seen between 13:00 to 16:00. Furthermore, as OEs are in *PQ* diagram, prosumers are able to control more intelligently. For example between 10:00 to 13:00, since this prosumer's BESS also participates in the voltage regulation, the injected power to the network is less than its net power. Therefore, according to its OE at that level of active power injection, reactive power compensation is not required. This essentially improves the power factor in the line, which leads to less transmission loss. In addition, it should be noted that a few times this prosumer's OEs allow higher generation. However, due to its limit (PV systems capacity limit as well as its reactive power capability limit (18)), it cannot generate more than a certain value.

In terms of BESS's charging and discharging, Fig. 13 shows house 40A's BESS's SoC with respect to its net power. It can be seen that using the proposed prosumer algorithm results in the slower charging as BESSs mostly charge when $P_{cur}^{40A,t} \geq 0$. Nonetheless, due to the high amount of the surplus generated power, it is fully charged before 13:00. This shows that the capacity of the BESS is not sufficient to absorb the surplus active power completely. Moreover, as the discharge power with and without OEs are calculated similarly, in both cases the discharging curve is the same. The BESS meets the demand plus a fixed value ($0.1 \times \overline{P}_d^{40A} = 400$W), so it will be fully discharged for the next day.

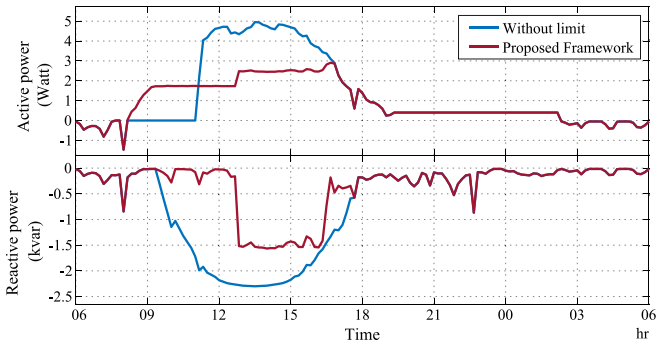

Fig. 12. Prosumer 40A's active and reactive power when prosumers are/are not provided with OEs.

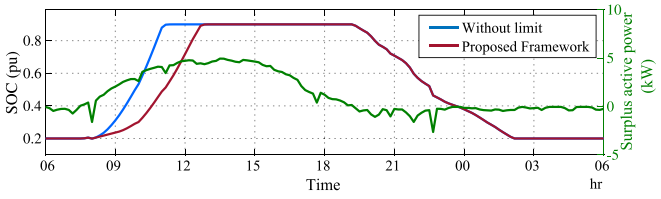

Fig. 13. Prosumer 40A's (left) BESS's SoC when prosumers are/are not provided with OEs (right) surplus active power (P_{net}^{40A}).

4.2. Case study 2: Comparative analysis with the fixed limit approach

In this case study, it is considered that instead of dynamic OEs prosumers are provided with a fixed limit for the output active power. Since there is only one limit for the active power, prosumers with reactive power capability use the droop curve shown in Fig. 5 to control the reactive power. For this network, by assigning the limit to 2.25 kW, all limits will be almost meet. As shown in Figs. 14 and 15, this approach keeps almost all customers' voltage magnitude and lines' loading within the permissible band. However, since the fixed limit is non-dynamic (loads variations are not considered), and does not consider the generation unbalance in phases, this approach is too conservative and the complete capacity of the network is not used. In another word, none of the voltage and current limits of the network are not reached. This can be seen especially in the voltage magnitude of customers connected to phase *C*, in which there is still at least 0.01 pu gap to reach the voltage limit during the peak generation. For example, in the studied network, utilizing the proposed framework, the total generated active power in the network is 1.109 MWh, while it reduces to 0.976 MWh (12%↓) using the fixed limit. This shows that compared to the fixed limits, the proposed dynamic limits allows more PV generation (less curtailment) in the network. In Table 4 the summary of simulation *Case Study1* and *Case Study1* are illustrated.

4.3. Case study 3: Scalability of the DNO algorithm

In terms of the practical applicability, the scalability of the DNO algorithm is the most important feature as it has to deal with a large number of prosumers. To study this, the computation time of the proposed DNO algorithm has been calculated for networks with different numbers of customers and prosumers using a PC with an i7-8700K processor and 32 GB of RAM. The results are shown in Fig. 16 alongside the linear regression. It can be seen that for the studied network with 55 houses, in each time step, DNO only needs 0.1098 s for the calculation. While, for a larger network, for example with 100 houses, the required calculation time is around 0.12 s. This shows that the DNO calculation time is insignificant compared to the dynamics of solar irradiance changes.

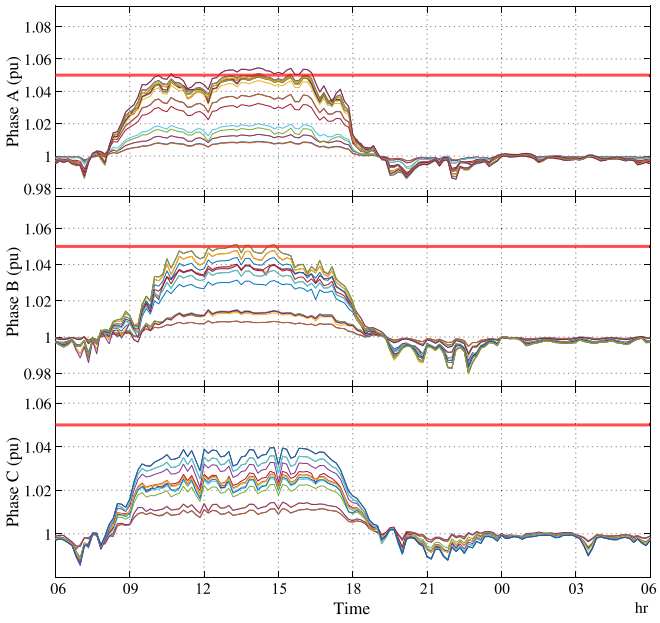

Fig. 14. Maximum phase voltage unbalance factor of the network when prosumers are provided with a fixed limit.

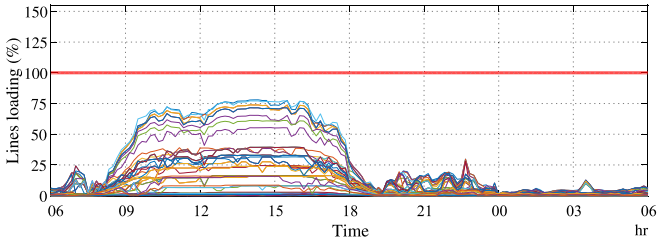

Fig. 15. Maximum phase voltage unbalance factor of the network when prosumers are provided with a fixed limit.

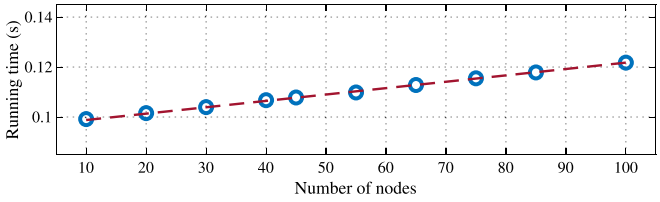

Fig. 16. The running time of DNO's algorithm.

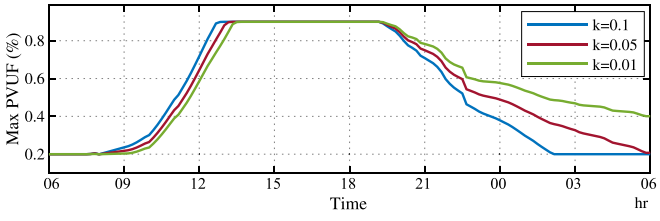

Fig. 17. The SoC of BESS of 40A for k= 0.1, k= 0.05, and k= 0.01.

4.4. Case study 4: Sensitivity analysis of k^h

The impact of different values of k^h on the performance of the proposed prosumer algorithm (Algorithm 3) is further studied. To this end, three values of k^h, 0.1, 0.05, and 0.01 are considered in the network of *Case Study 1*. Fig. 17 shows the SoC of the BESS installed in house 40A. It can be observed that the lower values of k result in slower charging and discharging. Insofar, for $k = 0.01$, the battery is not fully discharged, therefore it will not be able to absorb the curtailed active power in the next day to its maximal extent. This does not endanger the integrity of the network however, the prosumer will not profit to its maximal extent.

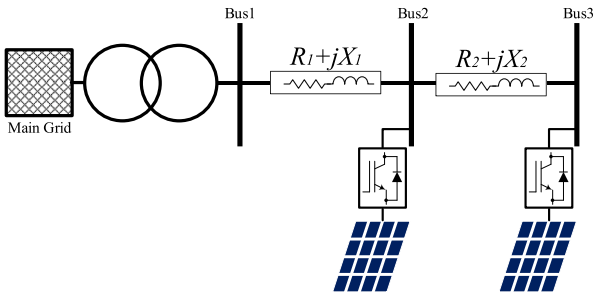

Fig. 18. Three-bus LV feeder line diagram [24].

5. Comparative analysis with the state of the art

In this section, the proposed method has been compared with a state of the art method [24]. Both the proposed method and [24] have a similar framework. First, in each time interval, DNO collects the prosumers' intended active and reactive power. Then, the DNO calculates an OE for each prosumer and broadcast it. While in [24] the OEs are only determined for the active power, the calculated OEs in the proposed method provide both active and reactive power limits. For comparison, the three-bus network (see Fig. 18) from [24] has been used to compare the methods. In this network, two prosumers with a 5kWp PVSS are connected to buses 2 and 3, respectively. However, to study the impact of PQ OEs on the total generation in the grid (or curtailment), it is considered that they do not have a BESS. Similar to [24], for the sake of simplicity, the same 24-hour net demand profile (adopted from [36]) is considered for both prosumers (see Fig. 19). Furthermore, $R_1 = R_2 = 0.34$ Ohm.

To study the impact of reactive power, five different values of R/X have been used. The range of the R/X values are adopted from [32]. Moreover, the performance of the proposed method has been investigated for two cases; with a 10% oversized inverter, and without oversizing the inverter. As Table 5 shows, the proposed method, even in a high R/X ratio and without oversizing the inverter, can increase the total generated active power in the network. Although, for the higher value of R/X its effectiveness diminishes. In terms of PVSSs' inverter oversizing, for lower R/X ratios of 1.3, and 2.4, oversizing does not impact the proposed method's performance. In these cases, PVSSs do not require to absorb a high amount of reactive power. Therefore, the freed-up capacity due to the active power curtailment is sufficient for reactive power compensation. On the other hand, for lower R/X ratios of 3.75, 4.5, and 6.3, it can be seen that when PVSSs' inverter are not oversized, the total generated active power reduces. This is due to the fact that the freed-up capacity of PVSSs is not sufficient, and they are only able to have limited reactive power compensation. Nonetheless, there is still a noticeable improvement in terms of generated active power compared to [24].

6. Conclusions

In this paper, a novel control framework has been proposed to avoid nodes' over-voltage and lines' over-current issues in distribution networks with high penetration of DERs. In this framework, the distribution network operator (DNO) routinely provides prosumers with

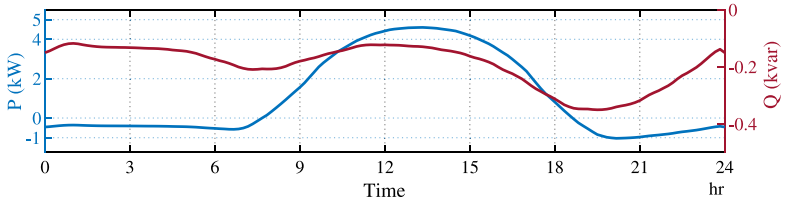

Fig. 19. Prosumers intended active and reactive power.

Table 5
Comparison of the proposed method with [24].

		Total generated active power (kWh)		
		Proposed method		[24]
		10% oversizing	Without oversizing	
R/X ratio	1.3	51.89	51.89	34.33
	2.4	45.20	45.20	33.60
	3.75	41.03	39.55	33.28
	4.5	39.71	38.16	33.19
	6.3	37.78	36.19	33.06

the operating envelops (OEs), while prosumers decide to control their assets taking in account these OEs. Hence, there is no need for the DNO to directly control prosumers' DERs. Unlike the existing works, the proposed dynamic OEs are defined in the *PQ* diagram to cover all types of prosumers, particularly prosumers with reactive power control capability. Furthermore, an algorithm for prosumers is introduced so they are able to control their PVSS and BESS accordingly. Simulation case studies using the IEEE European low-voltage test feeder for a PV-rich network are carried out, and the results show that the proposed framework enables prosumers to use their DERs without violating the voltage and current limits in the network. The comparison of results with the fixed limit method shows 12% increase in prosumers injection to the grid as the network hosting capacity is fully utilized. Furthermore, the DNO algorithm in terms of applicability and scalability is analyzed for networks with different number of prosumers, which proves its suitability for large-scale networks. Finally, the proposed *PQ* OE is compared with the state of the art and it is shown that using this method results in more generation in the network compared to the one-dimensional active power OEs.

CRediT authorship contribution statement

Yasin Zabihinia Gerdroodbari: Conceptualization, Methodology, Visualization, Writing – original draft. **Mohsen Khorasany:** Conceptualization, Methodology, Visualization, Writing – original draft. **Reza Razzaghi:** Conceptualization, Supervision, Resources, Writing – review & editing, Project administration.

Declaration of competing interest

The authors declare that they have no known competing financial interests or personal relationships that could have appeared to influence the work reported in this paper.

Acknowledgments

This work was supported by the Australian Commonwealth Scientific and Industrial Research Organization (CSIRO).

Appendix

In this paper, phase voltage unbalance factor in node n is calculated as:

$$PVUF^{n,t} = \frac{max(|V_a^{n,t} - \overline{V^{n,t}}|, |V_b^{n,t} - \overline{V^{n,t}}|, |V_c^{n,t} - \overline{V^{n,t}}|)}{\overline{V^{n,t}}}, \quad (24)$$

where $V_a^{n,t}$, $V_n^{n,t}$, and $V_c^{n,t}$ are the phase to neutral voltage magnitudes of each phase and $\overline{V^{n,t}}$ is their average at time t [37].

References

[1] Razavi S-E, Rahimi E, Javadi MS, Nezhad AE, Lotfi M, Shafie-khah M, et al. Impact of distributed generation on protection and voltage regulation of distribution systems: A review. Renew Sustain Energy Rev 2019;105:157–67.
[2] Howlader AM, Sadoyama S, Roose LR, Chen Y. Active power control to mitigate voltage and frequency deviations for the smart grid using smart PV inverters. Appl Energy 2020;258:114000. http://dx.doi.org/10.1016/j.apenergy.2019.114000.
[3] Gerdroodbari YZ, Razzaghi R, Shahnia F. Decentralized control strategy to improve fairness in active power curtailment of PV inverters in low-voltage distribution networks. IEEE Trans Sustain Energy 2021;12(4):2282–92. http://dx.doi.org/10.1109/TSTE.2021.3088873.
[4] Jain AK, Horowitz K, Ding F, Sedzro KS, Palmintier B, Mather B, et al. Dynamic hosting capacity analysis for distributed photovoltaic resources—Framework and case study. Appl Energy 2020;280:115633. http://dx.doi.org/10.1016/j.apenergy.2020.115633.
[5] Chen C-S, Lin C-H, Hsieh W-L, Hsu C-T, Ku T-T. Enhancement of PV penetration with DSTATCOM in taipower distribution system. IEEE Trans Power Syst 2012;28(2):1560–7.
[6] Hashemi S, Østergaard J, Degner T, Brandl R, Heckmann W. Efficient control of active transformers for increasing the PV hosting capacity of LV grids. IEEE Trans Ind Inform 2016;13(1):270–7.
[7] Ciocia A, Boicea VA, Chicco G, Di Leo P, Mazza A, Pons E, et al. Voltage control in low-voltage grids using distributed photovoltaic converters and centralized devices. IEEE Trans Ind Appl 2019;55(1):225–37. http://dx.doi.org/10.1109/TIA.2018.2869104.
[8] Sun X, Qiu J, Zhao J. Optimal local volt/var control for photovoltaic inverters in active distribution networks. IEEE Trans Power Syst 2021;36(6):5756–66. http://dx.doi.org/10.1109/TPWRS.2021.3080039.
[9] Wang L, Bai F, Yan R, Saha TK. Real-time coordinated voltage control of PV inverters and energy storage for weak networks with high PV penetration. IEEE Trans Power Syst 2018;33(3):3383–95. http://dx.doi.org/10.1109/TPWRS.2018.2789897.
[10] Alyami S, Wang Y, Wang C, Zhao J, Zhao B. Adaptive real power capping method for fair overvoltage regulation of distribution networks with high penetration of PV systems. IEEE Trans Smart Grid 2014;5(6):2729–38. http://dx.doi.org/10.1109/TSG.2014.2330345.
[11] Wang Y, Tan KT, Peng XY, So PL. Coordinated control of distributed energy-storage systems for voltage regulation in distribution networks. IEEE Trans Power Deliv 2016;31(3):1132–41. http://dx.doi.org/10.1109/TPWRD.2015.2462723.
[12] Riffonneau Y, Bacha S, Barruel F, Ploix S. Optimal power flow management for grid connected PV systems with batteries. IEEE Trans Sustain Energy 2011;2(3):309–20. http://dx.doi.org/10.1109/TSTE.2011.2114901.
[13] Zhang B, Lam AY, Domínguez-García AD, Tse D. An optimal and distributed method for voltage regulation in power distribution systems. IEEE Trans Power Syst 2015;30(4):1714–26. http://dx.doi.org/10.1109/TPWRS.2014.2347281.
[14] Gebbran D, Mhanna S, Ma Y, Chapman AC, Verbič G. Fair coordination of distributed energy resources with volt-var control and PV curtailment. Appl Energy 2021;286:116546. http://dx.doi.org/10.1016/j.apenergy.2021.116546.
[15] Olivier F, Aristidou P, Ernst D, Van Cutsem T. Active management of low-voltage networks for mitigating overvoltages due to photovoltaic units. IEEE Trans Smart Grid 2016;7(2):926–36. http://dx.doi.org/10.1109/TSG.2015.2410171.
[16] Khorasany M, Razzaghi R, Gazafroudi AS. Two-stage mechanism design for energy trading of strategic agents in energy communities. Appl Energy 2021;295:117036. http://dx.doi.org/10.1016/j.apenergy.2021.117036.

[17] Iria J, Scott P, Attarha A, Gordon D, Franklin E. MV-LV network-secure bidding optimisation of an aggregator of prosumers in real-time energy and reserve markets. Energy 2022;242:122962. http://dx.doi.org/10.1016/j.energy.2021.122962.

[18] Bridge J. Export Limits for Embedded Generators up to 200 kVA Connected at Low Voltage. AusNet Services; 2017.

[19] evolve DER project. On the calculation and use of dynamic operating envelopes. 2021, URL https://arena.gov.au/assets/2020/09/on-the-calculation-and-use-of-dynamic-operating-envelopes.pdf.

[20] Advanced VPP Grid Integration. Analysis of the vpp dynamic network constraint management. 2021, URL https://arena.gov.au/assets/2021/01/analysis-of-the-vpp-dynamic-network-constraint-management.pdf.

[21] Project EDGE (Energy Demand and Generation Exchange). Project edge lessons learnt 1. 2021, URL https://arena.gov.au/assets/2021/05/project-edge-lessons-learned-report-1.pdf.

[22] Optimal DER Scheduling for Frequency Stability. Optimal der scheduling for frequency stability study report. 2022, URL https://arena.gov.au/assets/2022/03/optimal-der-scheduling-for-frequency-stability-study-report.pdf.

[23] Petrou K, Liu MZ, Procopiou AT, Ochoa LF, Theunissen J, Harding J. Managing residential prosumers using operating envelopes: An Australian case study. In: Proceedings of the CIRED Workshop, Berlin, Germany. 2020, p. 22–3.

[24] Petrou K, Procopiou AT, Gutierrez-Lagos L, Liu MZ, Ochoa LF, Langstaff T, et al. Ensuring distribution network integrity using dynamic operating limits for prosumers. IEEE Trans Smart Grid 2021;1. http://dx.doi.org/10.1109/TSG.2021.3081371.

[25] Bennett CJ, Stewart RA, Lu JW. Development of a three-phase battery energy storage scheduling and operation system for low voltage distribution networks. Appl Energy 2015;146:122–34. http://dx.doi.org/10.1016/j.apenergy.2015.02.012.

[26] Advanced Planning of PV-Rich Distribution Networks Study. Advanced planning of PV-rich distribution networks – deliverable 3: traditional solutions. 2020, URL https://arena.gov.au/assets/2019/02/advanced-planning-of-pv-rich-distribution-networks-deliverable-3-traditional-solutions.pdf.

[27] Donald and Tarnagulla Microgrid Feasibility Study. Area hosting capacity assessment, project number: 04. 2021, URL https://c4net.com.au/wp-content/uploads/2021/05/4.-Area-Hosting-Capacity-Assessment_Report-Final.pdf.

[28] Victorian distribution network service provider (DNSP) basic micro EG connections power quality response mode settings. 2019, URL https://www.ausnetservices.com.au/-/media/Files/AusNet/New-Connections/20191023--Power-Quality-Response-Mode-SettingsFINAL.ashx?la=en.

[29] Han S, Han S, Aki H. A practical battery wear model for electric vehicle charging applications. Appl Energy 2014;113:1100–8.

[30] Wang L, Yan R, Bai F, Saha T, Wang K. A distributed inter-phase coordination algorithm for voltage control with unbalanced PV integration in LV systems. IEEE Trans Sustain Energy 2020;11(4):2687–97. http://dx.doi.org/10.1109/TSTE.2020.2970214.

[31] Tushar W, Saha TK, Yuen C, Azim MI, Morstyn T, Poor HV, et al. A coalition formation game framework for peer-to-peer energy trading. Appl Energy 2020;261:114436.

[32] IEEE European low voltage test feeder. 2019, URL https://site.ieee.org/pes-testfeeders/resources/.

[33] Safayet A, Fajri P, Husain I. Reactive power management for overvoltage prevention at high PV penetration in a low-voltage distribution system. IEEE Trans Ind Appl 2017;53(6):5786–94. http://dx.doi.org/10.1109/TIA.2017.2741925.

[34] LG chem catalog. 2018, URL https://www.lgchem.com/upload/file/product/LGChem_Catalog_Global_2018.pdf/.

[35] AS/NZS Standard 47772:2015. Grid connection of energy systems via inverters-Part 2: inverter requirements. 2015.

[36] Sharma V, Haque MH, Aziz SM. PV generation and load profile data of net zero energy homes in south Australia. Data Brief 2019;25:104235. http://dx.doi.org/10.1016/j.dib.2019.104235.

[37] Zabihinia Gerdroodbari Y, Razzaghi R, Shahnia F. Improving voltage regulation and unbalance in distribution networks using peer-to-peer data sharing between single-phase PV inverters. IEEE Trans Power Deliv 2021;1. http://dx.doi.org/10.1109/TPWRD.2021.3113011.